The Engineering Society
For Advancing Mobility
Land Sea Air and Space

400 COMMONWEALTH DRIVE WARRENDALE, PA 15096

# SAE Technical Paper Series

870816

# Intra-Cylinder Combustion Pressure Sensing

**J. E. Morris**
EE/Watson School
SUNY-Binghamton, NY

Earthmoving Industry Conference
Peoria, Illinois
April 7-9, 1987

870816

# Intra-Cylinder Combustion Pressure Sensing

**J. E. Morris**
EE/Watson School
SUNY-Binghamton, NY

ABSTRACT

At present, combustion pressure sensors find widespread use in basic engine research and development. In the future they could provide the essential information for closed loop engine control (of both fuel mixture and ignition timing) and diagnostics. The quartz piezoelectric device is the most familiar; its concept has been extended to piezo-ceramic configurations seated beneath or inside a sparkplug. This paper presents preliminary results for a novel fiber-optic pressure sensor incorporated into a spark-plug. Head-stud transducers are also described.

THE P-V DIAGRAM FOR AN IDEALIZED COMBUSTION CYCLE and its corresponding pressure crank-angle plot are shown in figure 1, along with a simple engine crank geometry. The P-$\theta$ diagram is similar to the P-t variation, provided that one can neglect the angular deceleration and acceleration as the piston approaches and passes TDC (top-dead-center) at 0°. Obviously, the pressure variation with time (P-t) can give complete thermodynamic information on the combustion cycle by incorporating both the crank geometry and instantaneous angular velocity (i.e. $\theta$-t) converting t to $\theta$ and then to V. For research purposes, these calculations can be performed routinely by a computer, either in real-time or on stored data. The approximation that the P-t waveform can be regarded as directly representative of the P-$\theta$ variation neglects a $\pm$1.5% variation in angular velocity at idle (1)*, a variation which increases with load.

In principle, the P-t signal could be used for real-time engine control or for on-line diagnostics by performing the same transformation (t to $\theta$ to V) by microprocessor as done in the laboratory. In practice, the computational overhead, while feasible, is unnecessary. Control algorithms, for example, routinely employ empirical target criteria and diagnostics can similarly compare measurement to preset limits.

It does not require a great deal of imagination to see that the integrated torque delivered by a given pressure waveform (i.e. one of a given shape and amplitude) will depend upon its position in time (or angle.) At one extreme, a symmetrical pressure pulse centered at TDC obviously delivers no net torque to the drivetrain. There is clearly some optimum position $\theta_m$ for the pressure peak, and this will be equally so for an asymmetrical pulse. Possibly, then, maximum output may be assured by controlling the pressure peak position to this optimal $\theta_m$. The critical assumption here is that the pressure waveform's shape does not change appreciably with the many engine variables (load, rpm, temperature, etc.), but the empirical result that optimal spark ignition timing does in fact lead to a single peak pressure angle regardless of other engine parameters (2, 3) validates the assumption. Heywood et al (2) found the optimum pressure peak position for a GM 5.6$\ell$ V-8 to lie at 17.2 $\pm$ 1.2° ATDC with all variations of compression ratio, fuel mixture, rpm, percent EGR, load and combustion duration. Randall and Powell (3) obtained a figure closer to 20° ATDC for their CFR engine; the range of 15 to 20° is widely cited as typical (4). One must also realize that the waveform shape is only going to be reasonably constant with the peak occurring in about the right place. If the waveform P($\theta$) is known, the optimum peak angle $\theta_m$ can be found by

*Numbers in parentheses designate references at end of paper.

0148-7191/87/0407-0816$02.50

integrating torque $\tau(\Theta)$ over $\Theta$, where

$$\tau(\Theta) = P(\Theta)\, A \cos\Theta .\, R \cos(\pi/2 - \phi - \Theta)$$

$$= P(\Theta)\, AR \sin\Theta\, [1-\lambda^2 \sin^2\Theta + \lambda(1-\lambda^2)^{1/2}]$$

where $\lambda = R/L$. The approximation (5) that $\tau(\Theta) \simeq P(\Theta)\, AR \sin\Theta$ is subject to a 10 to 20% error for $\lambda = 0.1$ to 0.5.

We now have one criterion for an engine control algorithm: for all other variables fixed, (or controlled to optimal values by other means), one may be varied to bring the pressure peak position to its optimal value. In a spark ignition engine, the obvious parameter to control to this set point is ignition timing, which has been done both in the laboratory (6-8) and on the road (9,10). As a broad rule, the peak position shifts about 0.5° per degree change in ignition timing (9-11).

The other principal controllable engine input is fuel mixture, but here there are two different control strategies depending upon whether a stoichiometric or lean-limit mixture is required.

Lean-limit mixture control has been demonstrated in systems based on measurement of the dispersion in angular rotation times (8-10, 12-13). As fuel mixture approaches the lean-limit, statistical fluctuations between successive combustion qualities produce measureable variations in combustion pressure peak amplitude, position, time integral, etc. (2) with consequent fluctuations in the resultant delivered torque and angular acceleration. Monitoring the rotation times takes the end result of this sequence. It would be more direct to take the same information from some dispersion in the pressure waveform, and essentially any of the three parameters mentioned above - peak magnitude, position or area, (or even position of maximum rate of rise dP/dt)- could be used (2).

Stoichiometric mixture control from such a sensor is much more difficult than lean limit. It could be based on virtually any amplitude measurement on the pressure waveform. Peak amplitude is the most obvious choice, although area or maximum rate of rise are alternatives in principle. Such a control system must assume consistent waveform shape, of course, as for timing control, and therefore implies simultaneous successful ignition control. The problem is encountered in the correction strategy, since stoichiometry, unlike the lean-limit, can be approached from two sides. A dither technique would, presumably, be required to implement this type of control.

Combustion pressure measurement may, then, see development for both mixture and timing control from one sensor. Installation of sensors on all cylinders would furthermore provide a means for the correction of fuel maldistribution, which becomes a major problem in lean-limit engines. Spark inhibition also provides a method of calibration of the position of the crankshaft reference by accurately locating TDC as the pressure peak position without combustion. Still more related applications can be envisaged (11).

One of the sensors to be described below has been studied for the purpose of knock detection (6). Pressure fluctuations due to the oscillating pressure wavefront have a characteristic frequency which depends on combustion chamber geometry but is usually around 5KHz. Knock detection is required for maximum advance (knock limit) ignition strategies.

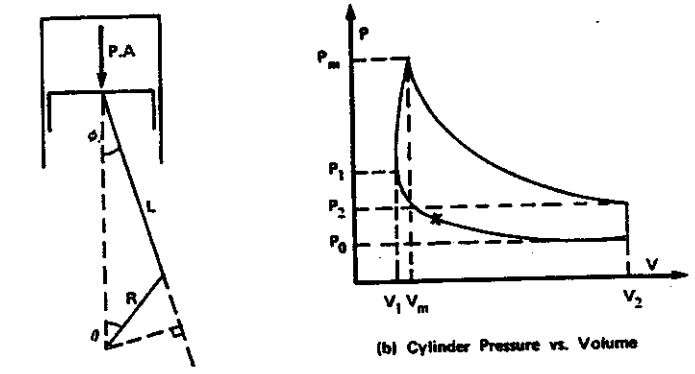


(a) Engine Crank Geometry

(b) Cylinder Pressure vs. Volume

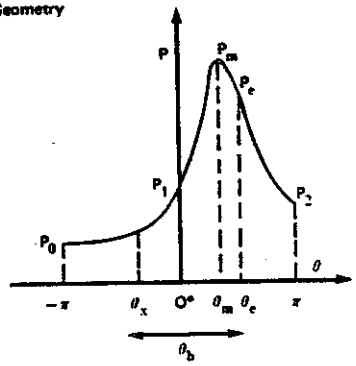


(c) Cylinder Pressure vs. Crank Angle

Figure 1
Cylinder pressure: thermodynamics and waveform.

QUARTZ PIEZOELECTRIC

The most commonly used combustion pressure sensors are commercial devices based on a piezoelectric quartz element (14, 15). Two versions are available. The first (figure 2(a)) requires a dedicated aperture into the combustion chamber, which is only available on research engines at this point. The quartz element is a mechanically resonant system, but with a resonant frequency typically around 100KHz (for these applications), which is well above fundamental frequencies of interest in either the combustion pressure pulse or knock signals. For all practical purposes, then, the sensor's source impedance may be regarded as capacitive.

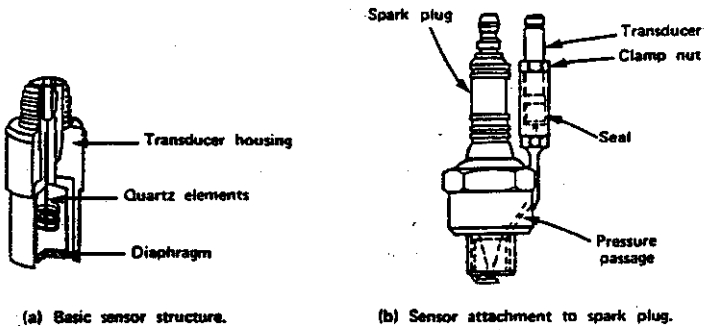


(a) Basic sensor structure. (b) Sensor attachment to spark plug.

Figure 2
Quartz combustion pressure sensors.

Figure 3(a) shows the mechanical resonant system of natural response determined by

$$m\frac{d^2x}{dt^2} + k\frac{dx}{dt} + sx = 0$$

For piezoelectric charge q proportional to displacement x ($q = \lambda x$)

$$\frac{m}{\lambda}\frac{d^2q}{dt^2} + \frac{k}{\lambda}\frac{dq}{dt} + \frac{s}{\lambda}q = 0$$

or (figure 3(b))

$$L\frac{di}{dt} + Ri + \frac{1}{C}\int i\,dt = 0$$

At low frequencies, force F = P x A area may be approximated by

$$F = sx = \frac{s}{\lambda}q = \frac{s}{\lambda}Cv$$

i.e. a maximum output signal voltage, v

$$v = \frac{\lambda}{C}\frac{F}{s}$$

requires maximum surface displacement, i.e. small s, a large charge/displacement ratio $\lambda$ and small sensor capacitance C. For quartz, $\lambda/s$ is nominally 2.26 pC/N. (14)

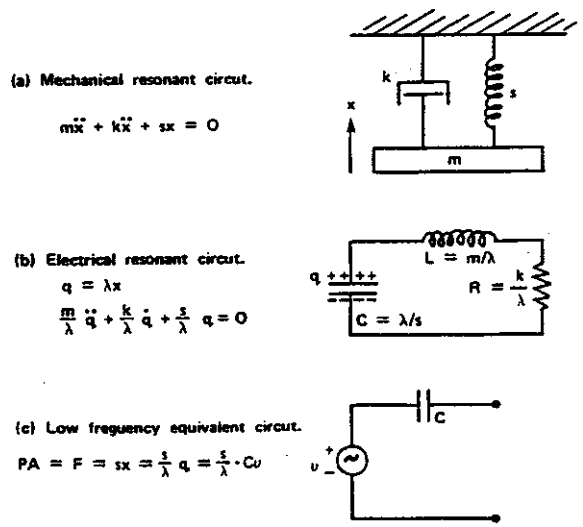


Figure 3
Piezo-electric transducer modeling.

The piezoelectric sensitivity of quartz falls off drastically above 200°C if standard crystal cuts are made, but the useful temperature range may be extended to 400°C by suitable special cuts(14). In the basic sensor, the quartz element is protected from the pressure chamber environment by a metal diaphragm (figure 1(a)). In the spark plug adapter, the same concept is used for the sensor itself, but connection from the chamber to the sensor is made through a narrow tube. This tube may introduce an additional resonance, typically at a much lower frequency than that of the quartz crystal. In general, the tube length must be kept as short as possible to keep tube resonance high, but the possibility exists of deliberately tuning the connector to the engine's characteristic knock frequency to increase the sensor's sensitivity to low knock levels. Lengths of 5 to 10 cm would be required for typical knock frequencies. The tube also blocks up with combustion products; while this is not a problem for research applications where engine runs are usually short and cleaning may be readily performed, it is obviously inappropriate for production road vehicles.

## PIEZO-CERAMIC SENSORS

Piezo-ceramic materials include barium titanate, various forms of lead zirconate/lead titanate and an increasing number of proprietary variations (16). While the range of material does offer the potential of higher signal outputs than are possible with quartz, other constraints generally mean that signal magnitudes are similar in practice. In particular one is restricted by the Curie temperature, beyond which the piezo-electric effect is lost. The real advantage of the piezo-ceramic material is that piezo-electricity is induced by poling in the final step of manufacture, after shaping. The unit cell dipoles are initially randomly oriented and the material is isotropic; anisotropy is produced by a high electric field which aligns the dipoles. Prior to poling, the ceramic piece may be produced in any shape suitable to its eventual application, (in contrast to the quartz crystal) with appropriate electrode deposition. Even after poling, the piezo-ceramic can be further machined for limited modification to other applications. It is this versatility which makes the piezo ceramic more attractive for the applications described below.

For production applications, intra-cylinder pressure sensing requires either a new engine design with an aperture dedicated to the purpose, or a sensor combined with some existing function, logically the spark-plug on SI engines.

A. Spark-Plug Washer

Kondo et al first proposed and demonstrated the installation of a piezo-ceramic sensor in the form of a washer under the spark-plug (17) as shown in figure 4(a). As fuel burns in the chamber, the pressure exerts an upward force on the plug housing, relieving the static pressure on the washer which was originally applied at insertion. One form of construction is shown in figure 4(b) (3,6,7,18) but the second shown in figure 4(c) is probably easier to build in a research lab. (9,10,19). In addition, grounding the sensor to the engine block at the plug can lead to ground-loop problems which are avoided with the twin-shielded format of figure 4(c). One of the difficulties encountered with positioning the sensor under the plug is that of making reliable contact to the sensor and removal or insertion of the device without breaking off the contact lead. One usually also wants the washer assembly to be as thin as possiible. It may be that the radial polarization and contact arrangement of figure 4(d) would allow a more robust mechanical construction.

In practice, the small quantities of prototype piezo-ceramic elements required by a research lab make the unit cost prohibitively expensive. For this reason, it is common to purchase standard sized disks of the required thickness and to cut the washer sensors from this stock. One may use either a sharp stainless steel tool (3) or a home-made grinder (10,19). In the latter method, the aluminum tool shown in figure 5 is used in an ordinary drill press running at its slowest speed. The piezo-ceramic stock is fastened to a plate with "5-minute" epoxy, the plate then being clamped to the drill's work-holder to minimize vibrations which can shatter the ceramic. A slurry of automotive valve grinding paste in water is maintained around the ceramic by a putty wall, or something similar, and the ring is slowly ground from the stock. Once the technique is acquired, breakages are rare. Once formed, the ring and residual stock may be removed from the plate by moderate heating. The grinding tool wears rapidly and needs periodic re-facing.

Piezo-ceramic washer sensors have been made as described above from disk stock supplied by Murata (Piezotite™ P-5) (20) and Philips (PXE-5) (21). (Crude devices have also been cut with scissors from piezo-ceramic door buzzer elements! They work, although the signal is small, but fail when the very low Curie temperature is exceeded on the engine.) Relevant data for the PXE-5 material (21) is presented in Table 1; the results presented below were obtained with PXE-5 stock. The Curie temperature was found to be

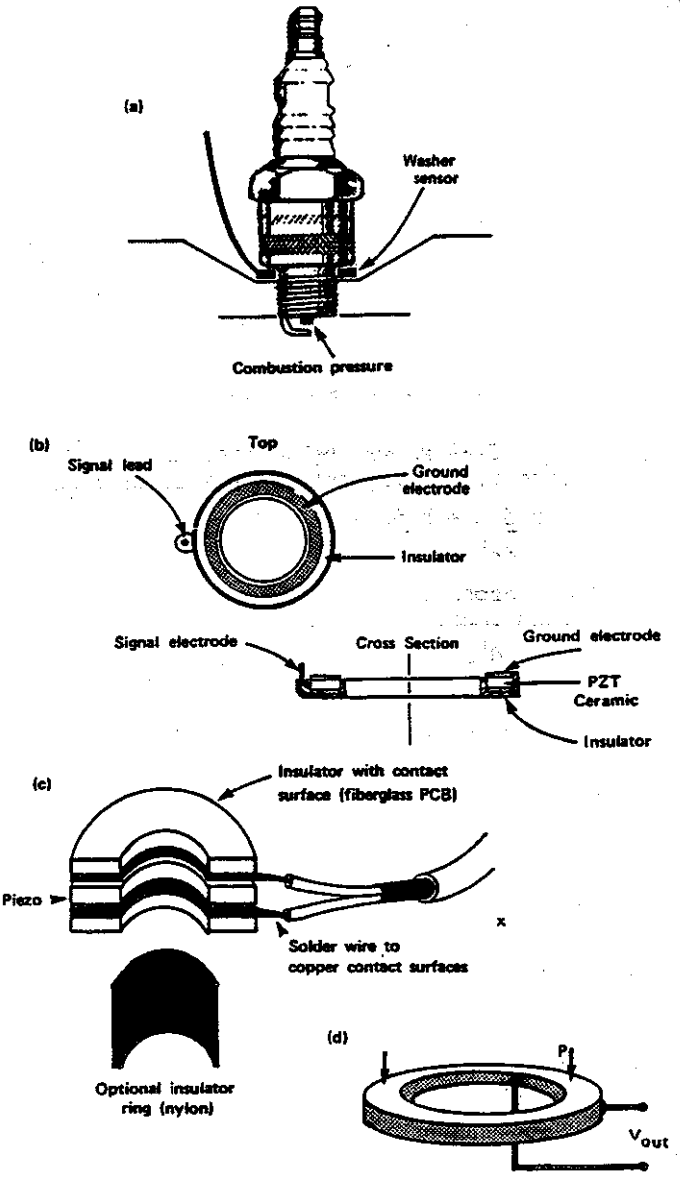


Figure 4

(a) Installation
(b) Construction: single wire and engine ground.
(c) Construction: twin coax, floating sensor, lab construction.
(d) Alternative poling.

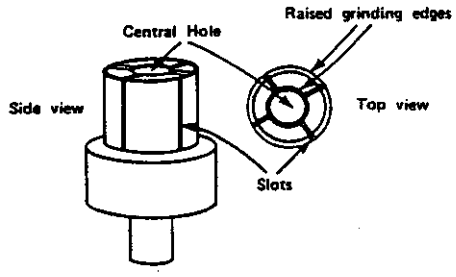


Figure 5

Aluminum Piezo Ring Grinding Tool

Table 1

Selected Properties of PXE-5 Piezo-ceramic(21)

| | |
|---|---|
| Curie temperature | 285°C |
| Compliance $S_{33}$ | $18.9 \times 10^{-12}$ $m^2/N$ |
| Poisson's ratio | 0.3 (approximately |
| Frequency constant | 1500-2000 Hz.m |
| Compressive strength | $>600 \times 10^6$ $N/m^2$ |
| Relative permittivity $\varepsilon_r$ | 1800 |
| Resistivity (25°C) | $10^{12}$ ohm.m |
| Dielectric loss factor (tan δ) | 0.016 at 1KHz |
| Piezoelectric voltage constants: | |
| $g_{33}$ | $24.2 \times 10^{-3}$ V.m/N |
| $g_{31}$ | $-10.7 \times 10^{-3}$ V.m/N |

adequate; no accurate measurement of the temperature at the base of the plug has been made. A typical intra-cylinder combustion pressure is about $7 \times 10^5$ $N/m^2$. Although only a fraction of that would be transmitted to the sensor, depending upon the mechanical coupling through the plug threads, it will be used below for estimating purposes. The compliance is small and there is negligible change in sensor dimensions. For a 1mm thick sensor, the resonant frequency

(1500 to 2000Hz.m ÷ $10^{-3}$m)

is of the order of MHz, and readily ignored for the present application. (Ignition system oscillations have been observed with frequencies around 5 to 10 KHz, also much lower than the sensor resonant frequency.) The compressive strength is adequate to survive the initial torque-down pressure necessary to provide dynamic signal range (remembering that combustion relieves sensor pressure) but is insufficient to withstand overly enthusiastic insertion. The plug should be "tweaked" down more gently than normal or its piezoelectric properties will be destroyed. Bulk resistivity can be neglected as a significant factor, dielectric loss being easily dominant, and potentially significant at high rpm. The most important parameter is the voltage constant. For a 1mm thick ring of 1mm width, the open circuit voltage for the pressure cited above is

$(7 \times 10^5\ N/m^2) \times (24.2 \times 10^{-3}\ Vm/N) \times (10^{-3}m)$

i.e., approximately 17 volts. (A more accurate result for the PXE-5 sensor, but following Randall and Powell's theoretical development (18), gives 9.4 volts (10).) In practice, some hundreds of millivolts are normally measured at idle with the devices described, going up to several volts under moderate load. From Table 1, $g_{33}$ was used above since the pressure and polarization were in the same direction. For the configuration of figure 4(d), $g_{31}$ would be used and the output signal is

$(7 \times 10^5\ N/m^2) \times (\Pi(1.2^2 - 1.0^2) \times 10^{-4} \div 4\ m^2) \times (10.7 \times 10^{-3}\ Vm/N) \times (10^{-3}m)/(\Pi \times 10^{-2} \times 10^{-3}\ m^2)$ for a

1mm thick 1cm i.d. ring, i.e. about 8.2 volts. (This difference is obviously related to Poisson's ratio.)

Sensor output is illustrated in figure 6, which also shows the effect of the ignition current pulse upon the sensor signal. This ignition noise is the biggest single problem with this type of sensor although it is not entirely unexpected with the ignition current flowing through the sensor ring, even if it is partially shielded by the steel of the spark plug shell. And in addition to ignition noise, the washer sensor picks miscellaneous mechanical noise from valve motion, vibration, etc. Another difficulty arises with the washer concept's unsuitability for tapered seat plugs.

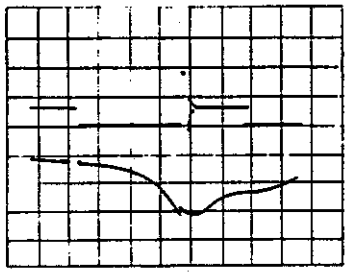

Figure 6
Coil ignition signal and piezo pressure peak (buffer output) with washer sensor.
Horiz.: 4ms/div
Vert.: 50 mV/div (pressure)

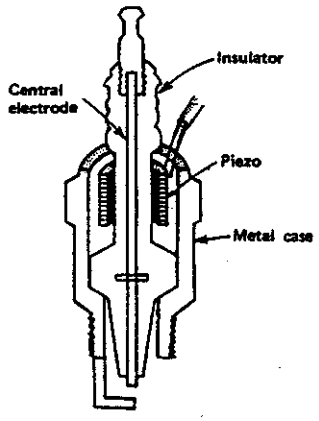


Figure 7
Cross-section of spark-plug containing internal sensor.

B. Internal Spark-Plug Sensor.

In an effort to resolve some of the difficulties described above, the piezo-ceramic sensor was put inside the spark-plug itself (figure 7).(19) Mechanical noise improved, and of course insertion difficulties were circumvented, but ignition noise was predictably worsened. However, one still has to deal with the ignition noise problem with the washer sensor, so the move inside the plug represents a net gain in performance.

The designer has a greater range of options with this configuration, covering both the means by which the combustion pressure is transmitted to the sensor, and the piezo-ceramic sensor geometry itself. There are two main pressure signal transmission concepts. The pressure tends to produce relative movement between the central electrode and the restrained spark plug shell, which may be translated into a piezo-ceramic signal either directly (as before) (figure 8(a)) or by a shearing action (figure 8(b)). Alternatively, the pressure may be transmitted to the interior cavity of the plug as a whole, either via a diaphragm (figure 8(c)), or by relative movement of electrode and shell (figure 8(d)), through an aperture between them (figure 8(e)). In the latter cases, a reduced output would be obtained as a result of the anisotropic properties, proportional to $|g_{33}| - |g_{31}|$, (figure 8(f)).

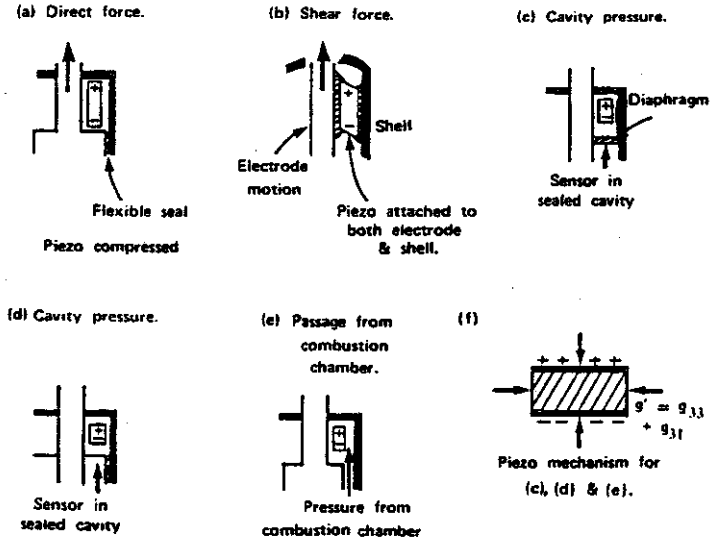


Figure 8
Pressure transduction to Piezo sensor inside plug cavity.

In building such sensors from plug components, it is essential to protect against the ejection of the central electrode from the plug when the cylinder fires. A screw cap may be fitted over the assembly to threads cut in the shell, or the shell may be turned over at the top with a hammer and punch after cutting with a hacksaw. In either case, a further cover (e.g. a board) should cover the plug in the engine as a further safety measure when working around it. The top end of the cavity must also be well sealed, care being taken that the sealant does not interfere with the piezo-ceramic's operation.

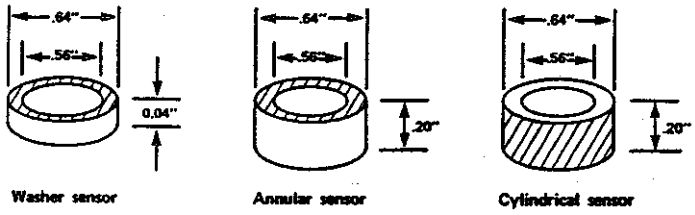


Figure 9
Sensor geometries (dimensions in inches).

Reference 19 compares the operation of three sensor geometries inside the plug,(figure 9) these being made of EC-64, the properties of which were tabulated (16,19). Waveforms are shown in figure 10 from two different sensors within the same cavity. Amplitudes are lower than normal and the ignition spike less obvious. The differentiated signal is the result of inadequate buffer impedance and shows accompanying noise enhancement.

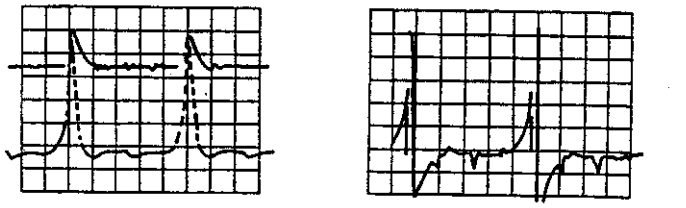

(a) Simultaneously measured cylinder pressure from the (upper) annular and (lower) cylindrical sensors.
Vertical axis (upper): 10 mV/Div
Vertical axis (lower): 0.5 mV/Div
Horizontal axis: 20 msec/Div

(b) A typical measured cylinder pressure trace showing differentiation with insufficient load impedance.
Vertical axis: 0.5 V/Div
Horizontal axis: 20 msec/Div

Figure 10
Pressure signals from internal spark-plug sensors.

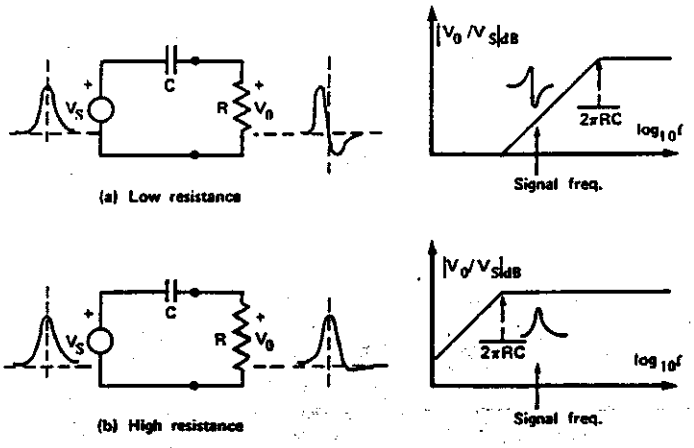


Figure 11
Effect of load resistance on signal differentiation.

C. Interfacing

The problem with a capacitive source is inherent differentiation by a resistive load (figure 11) unless RC is much greater than signal periods. Commercial interface systems employ a charge amplifier (figure 12) which avoids the problem provided all leakage resistances and the op amp input impedance (especially the common-mode input impedance $R_{i-cm}$ for the negative feedback configuration) are sufficiently high. For automotive combustion pressure sensing, the frequencies of interest are sufficiently low that one can achieve adequate RC time constants with conventional buffer circuits. In addition, it seems that the charge amplifier must be positioned right at the sensor, or else special cabling is required, since the standard input line becomes microphonic and picks up engine vibration noise.(10)

The essential functions of the interface buffer are to provide a faithful low impedance voltage output signal which is representative of the pressure waveform, and to reject (attenuate) the ignition noise. That is, a bandpass filter is required with the (unwanted) low-frequency roll-off well below frequencies of interest and the high-frequency one just above. The high frequency filtering could be of higher orders, but first order has been found to be adequate. An example of a buffer circuit and its output are shown in figure 13 for an internal spark-plug transducer, where the vestigial ignition "blip" has been deliberately left for demonstration purposes but could be totally eliminated by minor modification of the low pass filter on the output (19). Alternative circuits are shown in figure 14, which demonstrates the dependence of the sensor load impedance on source capacitance. In a potentially dirty (and noisy) environment, there are advantages to keeping resistances as low as possible. The trade-off in figure 14 is between the higher source capacitance (and lower load resistance) of (a) and the 2.4 times larger output signal from (b). Standard Norton op-amp buffer circuits have also been used with input and feedback resistors in the 10 Megohm range.(10)

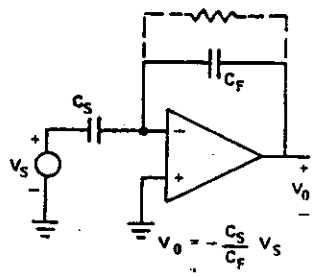


Figure 12
Charge amplifer.

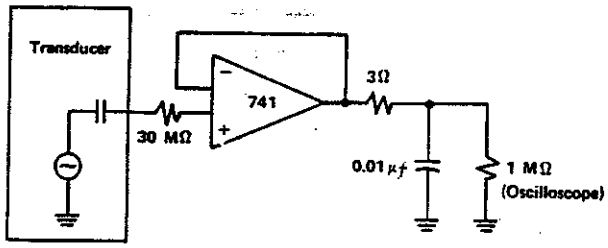


(a) Pressure signal buffer circuit: bandpass filter for no differentiation and ignition noise attenuation.

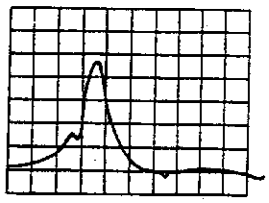

(b) Pressure signal output with reduced ignition spike
Vertical axis: 1.0 V/Div
Horizontal axis: 20 msec/Div

Figure 13
Interface buffer and output.

Once the low impedance output signal is obtained, further processing is possible. In particular, the peak position may be found by the circuit of figure 15.(10, 19) Note that the ignition noise must be completely eliminated or the circuit will trigger on it instead of the pressure peak. A peak position pulse can conveniently trigger a sample and hold system for A to D measurement of the peak height.

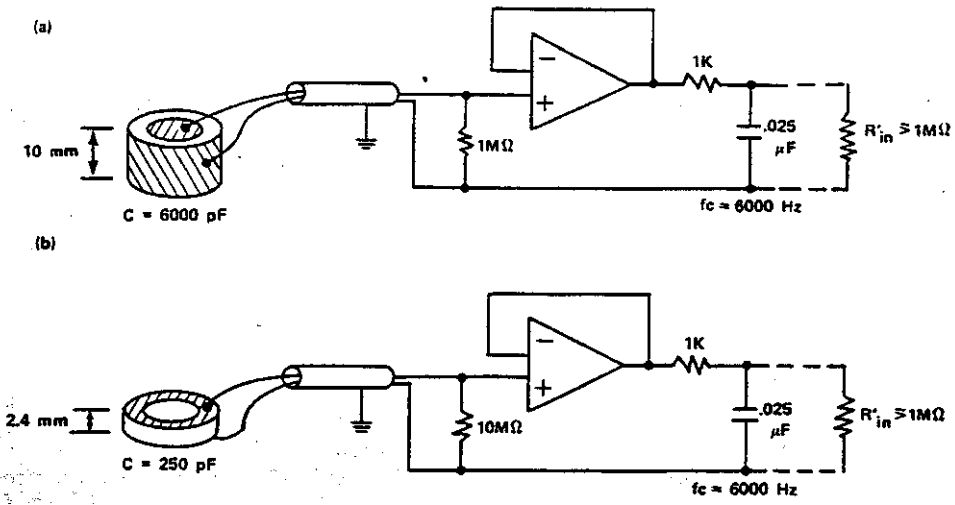


Figure 14
Design examples for 1mm thick sensors and (a) 1M, (b) 10M buffer impedances.

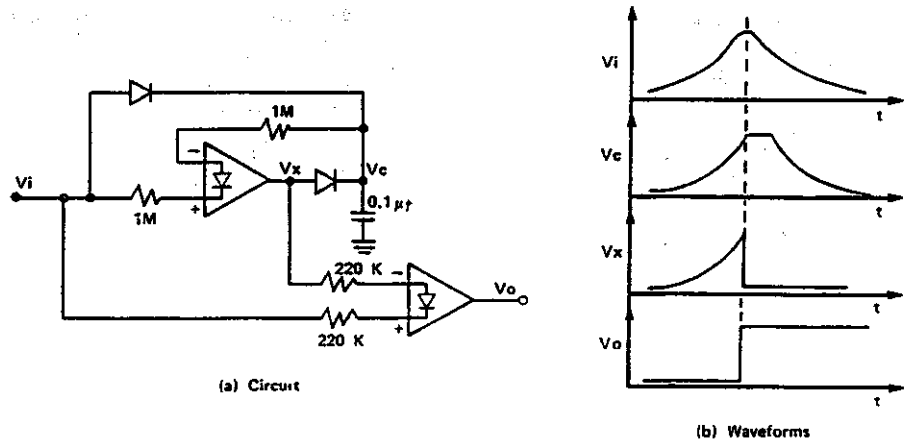


Figure 15
Peak position detector with two Norton amplifers.

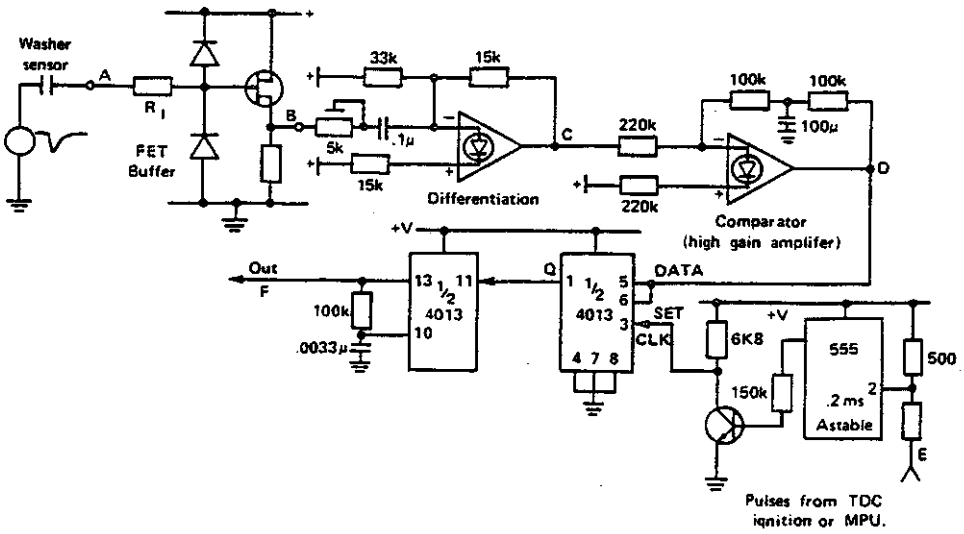


Figure 16
Piezo peak detection by zero–crossing.

Another circuit is shown in figure 16 with corresponding waveforms in figure 17 from a spark-plug washer sensor. The FET provides the buffer function; its output serves as a reference throughout figure 17. The peak detector is formed by a differentiator, the output of which crosses zero at the peak position, followed by a comparator (high gain amplifier) acting as a zero crossing detector. This is precisely the approach one would take with a noise-free signal and inspection of the waveforms of figure 17 confirms that the results only look sensible about the peak region. Elsewhere, and particularly during the ignition pulse, the output is inhibited by a gating signal, most conveniently derived from the ignition signal which causes the problem! At low load and rpm, the combustion pressure can fall to a point where the compression peak at TDC is comparable and a double peak develops, leading to a double pulse out (figure 18).

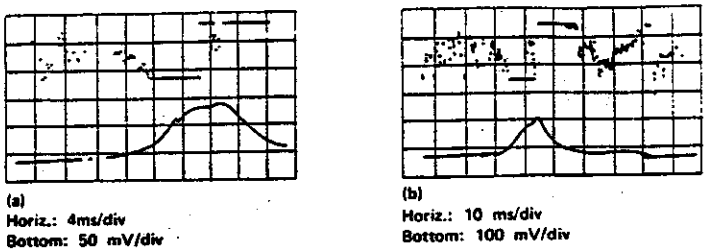

(a)
Horiz.: 4ms/div
Bottom: 50 mV/div

(b)
Horiz.: 10 ms/div
Bottom: 100 mV/div

Bottom: Buffered pressure signal B
Top: High gain differentiated signal (5V/div) D

Figure 18
Examples of double peaks at low load.

This system has been used on the road, with peak position pulses sent to a microcomputer and used to control the ignition timing in a feedback system based on optimal pressure peak position. A record of such control is shown in figure 19 where the control set-point has been changed from 20 to 12 to 17° ATDC as shown and the responses of the firing angle and pressure peak position are illustrated. (9,10) The spikes on the ignition angle trace are artifacts of a software fault (since corrected) but the scatter in peak position is real; ±5° dispersions have been observed by others.(11)

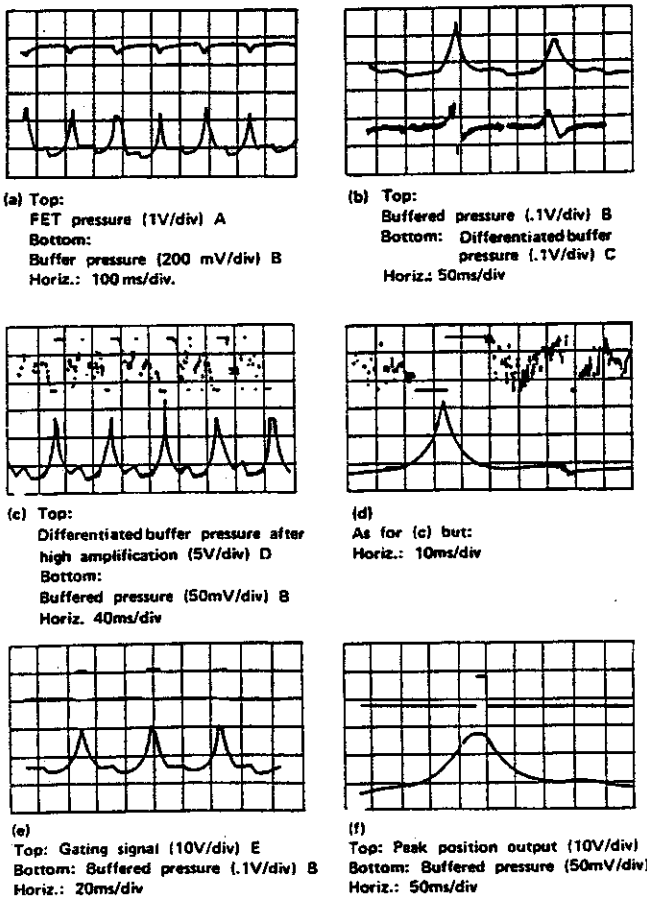

(a) Top:
FET pressure (1V/div) A
Bottom:
Buffer pressure (200 mV/div) B
Horiz.: 100 ms/div.

(b) Top:
Buffered pressure (.1V/div) B
Bottom: Differentiated buffer pressure (.1V/div) C
Horiz.: 50ms/div

(c) Top:
Differentiated buffer pressure after high amplification (5V/div) D
Bottom:
Buffered pressure (50mV/div) B
Horiz. 40ms/div

(d)
As for (c) but:
Horiz.: 10ms/div

(e)
Top: Gating signal (10V/div) E
Bottom: Buffered pressure (.1V/div) B
Horiz.: 20ms/div

(f)
Top: Peak position output (10V/div) F
Bottom: Buffered pressure (50mV/div)
Horiz.: 50ms/div

Figure 17
Circuit waveforms corresponding to points shown on Figure 16.

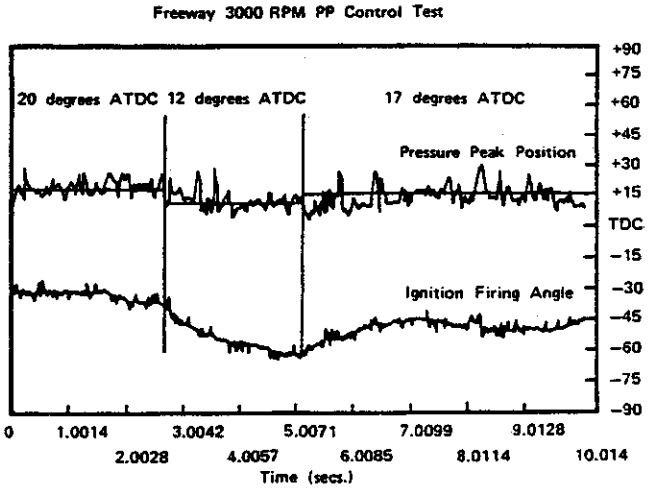


Figure 19
Ignition timing response to pressure peak control angle changes.

FIBER OPTIC SENSORS

With the main problem of the piezo-ceramic sensor being ignition noise pickup, it seems a logical step to move to a fiber-optic sensing and signal transmission system. The sensors described below are based on the micro-bending concept.

The basic principle is illustrated in figure 20, where the deformation of an optical fiber leads to light shedding from the guided wave where the conditions for total internal reflection are not maintained (22). A serrated plate may be used to deform the filter, or alternatively a spiral wound fiber (figure 21) may be sandwiched between parallel flat faces (23). The simple "circuit" is shown in figure 22.

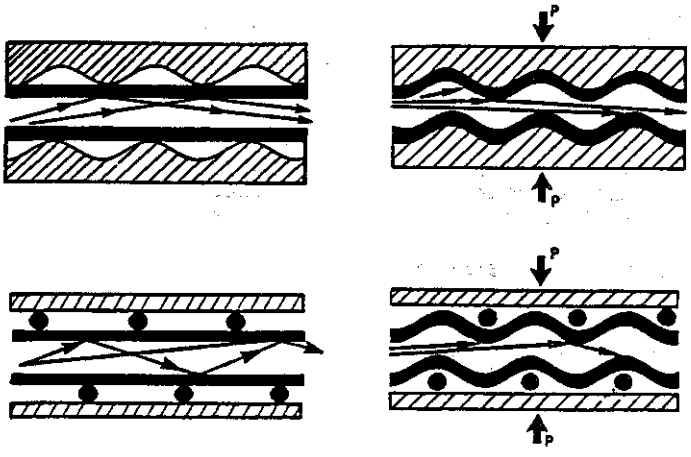


(a) Undeformed—light confined by internal relection.

(b) Deformed—light shedding at small angles of incidence.

Figure 20
The Microbending concept—light loss under deformation by pressure and serrated plates, or equivalent as shown.

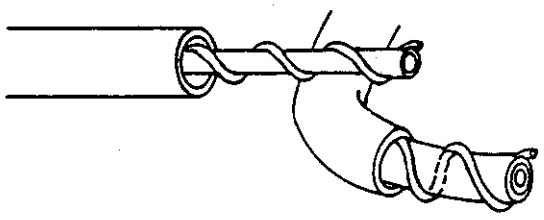

Figure 21
Spiral implementation of the microbending concept.

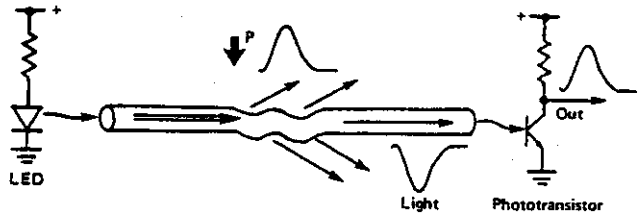


Figure 22
Electrical and optical circuits.

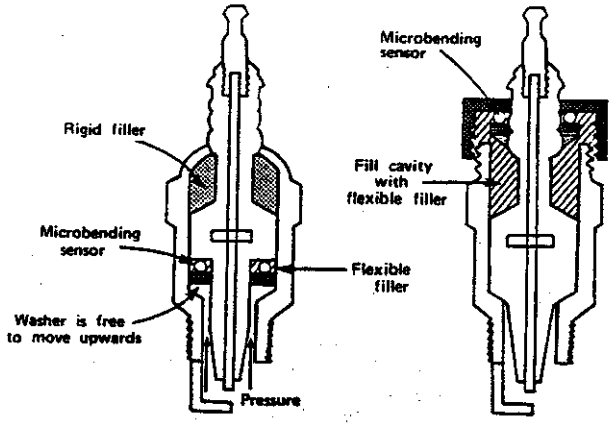


(a) Washer moves, compressing sensor against rigid plug assembly.

(b) Central electrode moves relative to shell, increasing microbending pressure.

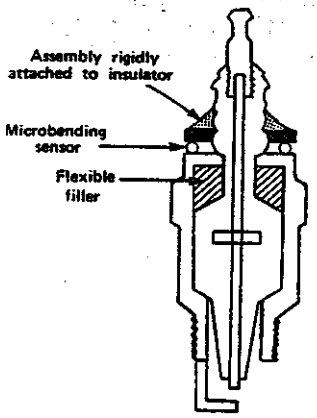


(c) Central electrode moves relative to shell, relieving microbending pressure.

Figure 23
Possible sparkplug sensor construction

Two spark-plug implementations have been tried to date, the first shown in figure 23(a), the second in figure 23(b) -both using spiral-wound fibers.(24) A third configuration is shown in figure 23(c) and many other variations upon these themes are possible. The key to these sensors is that a relatively large movement is required to adequately deform the fiber - roughly 0.04mm.(23) In figure 23(b) and (c), the central electrode must move by this amount relative to the plug shell, not a totally insignificant variation of the spark gap - although since it occurs after spark ignition this is not a serious problem in itself. The sensor compresses in figure 23(c) with relief of the (maximum) static pressure in figure 23(b). Cavity filler material must permit this movement.

The configuration of figure 23(a) is inherently preferable to the others since there is no movement of the spark-plug electrode, but one relies upon exposure of the sensing unit to the chamber pressure and upon the continued flexibility of the

high temperature filler which can be made to actually control the relationship between pressure and deformation, i.e. output. In the prototype built, the filler material properties were not optimized and a relatively small signal pulse of 50mV was obtained. This amplitude would increase considerably under load and is also controllable to some degree by light amplitude, phototransistor resistor, number of coil turns, etc.

An output from the sensor of figure 23(b) is shown in figure 24 and displays an embarrassingly large amplitude for a no-load signal. There is certainly considerable design leeway to play with here, possibly restricting electrode movement. The small fluctuations seen on the waveform are actually quantization noise; the waveform was digitally plotted after being recorded on an HP3561A Dynamic Signal Analyzer functioning as a digital oscilloscope. Note the absence of ignition noise!

Studies of thse fiber-optic sensors are continuing with mechanical design optimization, including mechanical resonance modeling. There are also other fiber optic configurations under consideration which may prove to be superior to those above.

HEADSTUD SENSORS

Piezo-ceramic washers have also been used under the headstud nuts of an engine (10). Combustion pressure pushes up against the cylinder head further compressing the washer beneath the nut. The signal is of comparable amplitude to that obtained from spark-plug washer sensors and is totally free of ignition noise. Mechanical noise level is acceptable. One particular advantage of the head-stud sensor is that one can pick up equal combustion signals from two cylinders on either side of its location. The problem with the sensors used was that the compressive strength of the piezo-ceramic was exceeded, very likely by torque-down during installation and before the additional combustion pressure load. One possible solution is to radically increase the piezo-ceramic washer area, to spread the load, but rough calculation suggests that the required area would be too large for convenience.

One solution to the problem might be to use quartz load washers (14).

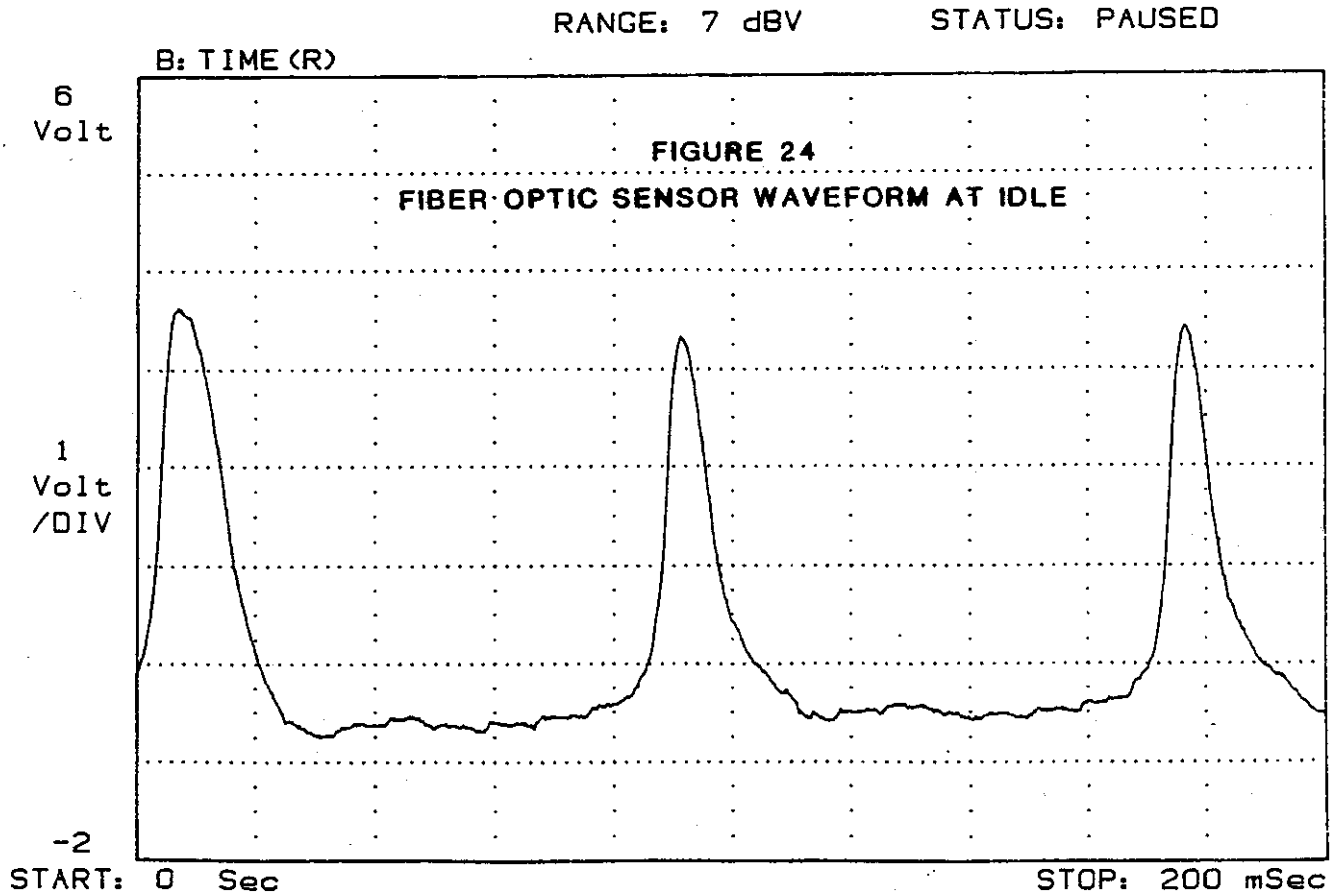


FIGURE 24
FIBER OPTIC SENSOR WAVEFORM AT IDLE

## CONCLUSIONS

Combustion pressure sensing has potential for engine diagnostics and control, providing both fuel mixture and ignition timing information. While the quartz transducer is still standard equipment in the laboratory, a cheaper and more adaptable unit is required for production applications. Piezo-ceramic elements have been used as spark plug, washers, inside spark plugs and under head-studs but suffer from admittedly surmountable noise problems. The fiber optic sensor is regarded as the preferred technique for eventual commercial development at this point.

Although the preceding discussion has referred entirely to spark-ignition engines and sensor placement around the spark-plug dominates the techniques, it will be obvious that comparable engine control algorithms and diagnostic techniques would be feasible in diesel engines. Furthermore, sensor placement within a glow-plug would be directly analogous to the spark-plug concept (with additional temperature problems but less constraint on motion), or even within a fuel injector.

## ACKNOWLEDGEMENTS

This work has depended over the years upon the assistance of various students, especially Roy Smith, Hugh Anderson, Malcolm Stewart, Li-Chi and Mohammad Khan.

## REFERENCES

1. J. E. Morris and T. C-C Chen, "PLL Sensing for Engine Diagnostics and Control," SAE Paper 850494

2. J. B. Heywood, J. M. Higgins, R. A. Watts and R. J. Tabaczynski, "Development and Use of a Cyclic Simulation to Predict SI Engine Efficiency and Knock Emissions," SAE Paper 790291

3. J. D. Powell, K. W. Randall and R. Hosey, "Closed Loop Cotnrol of Automotive Engines," Final Report, Contract DOT-OS-60151, Feb. 1978

4. C. F. Taylor, "The Internal Combustion Engine in theory and Practice," Vol. 2, MIT Press, 1968

5. C. K. Leung, U. S. patent 4,197,767, April 15, 1980

6. R. J. Hosey and J. D. Powell, "Closed Loop Knock Adaptive Spark Timing Control Based on Cylinder Pressure," ASME paper 78-WA/DSC-15

7. M. Hubbard, P. D. Dobson and J. D. Powell, "Closed Loop Control of Spark Advance Using a Cylinder pressure Sensor," ASME paper 75-WA/Aut.17

8. C. K. Leung and J. J. Schira, "Digital Analyzer for Internal Combustion Engines," SAE paper 820207

9. J. E. Morris, H. Anderson and R. Smith, "Retrofit Feedback Control of A/F Ratio and Ignition Timing for Fuel Economy," SAE Paper 820389

10. J. E. Morris, "Instrumentation of Cars for fuel Economy," Contract 3119, N.Z. Energy Research & Development Committee, (University of Auckland, N.Z.) Report No. 70 (and appendices), April 1982

11. S. R. Bhot and R. S. Quayle, "The Control of Ignition Timing to Achieve Maximum Fuel Economy," I Mech E Paper C174/81

12. M. D. Leshner, J. W. Stuart and E. Leshner, "Closed Loop Control for Adaptive Lean Limit Operation," SAE Paper 780039

13. M. D. Leshner, C. A. Luengo and F. Calandra, "Brazilian Experience with Self-Adjusting Fuel System for Variable Alcohol-Gasoline Blends," SAE Paper 800265

14. Kistler Instrument Corporation, Amherst, NY

15. PCB Piezotronics Inc., Depew, N.Y.

16. EDO Western Corp., Salt Lake City, Utah

17. M. Kondo, A. Niimi and T. Nakamura, "Indiscope - A New Combustion Pressure Indicator with Washer Transducers," SAE Paper 750883

18. K. W. Randall and J. D. Powell, "A Cylinder Pressure Sensor for Spark Advance Control and Knock Detection," SAE Paper 790139

19. J. E. Morris and Li-Chi, "Improved Intra-Cylinder Combustion Pressure Sensor," SAE Paper 850374

20. Murata North America, Inc., Marietta, GA

21. J. Van Randeraat and R. E. Setterington (Eds), "Piezoelectric Ceramics," Philips (1974)

22. EoTec Corp, West Haven, CT

23. Hergatite™, Herga Inc, Valley Forge, PA

24. M. Khan, "Fiber Optic Combustion Pressure Sensor," MSEE Thesis, SUNY-Binghamton (1986)